Journal of Inorganic and General Chemistry
ZAAC
Zeitschrift für anorganische und allgemeine Chemie
www.zaac.wiley-vch.de
RESEARCH ARTICLE
DOI: 10.1002/zaac.202200330

# $Li_3TrAs_2$ ($Tr$ = Al, Ga, In) – Derivatives of the antifluorite type structure, conductivities and electronic structures

Florian Wegner,[a] Franziska Kamm,[a] Florian Pielnhofer,[a] and Arno Pfitzner*[a]

*Dedicated to Prof. Wolfgang Schnick on the occasion of his 65th birthday.*

$Li_3AlAs_2$, $Li_3GaAs_2$ and $Li_3InAs_2$ were obtained from the elements via high temperature synthesis. $Li_3AlAs_2$ and $Li_3GaAs_2$ crystallize in a distorted 2·2·1 superstructure of the antifluorite structure type. The orthorhombic crystal structure is isotypic to $Li_3AlP_2$ and $Li_3GaP_2$, space group *Cmce* (No. 64) showing layers of condensed $TrAs_4$-tetrahedra ($Tr$ = Al, Ga). $Li_3InAs_2$ crystallizes isotypic to $Li_3InP_2$ in a distorted 2·2·4 antifluorite type superstructure. The crystal structure is tetragonal, space group $I4_1/acd$ (No. 142), showing a 3D-network of $In_4As_{10}$-supertetrahedra. Structural characterization by powder X-ray diffraction, thermal analysis, conductivity measurements and band structure calculations show ion conductivity for $Li_3InAs_2$ and electronic charge transport for $Li_3AlAs_2$ and $Li_3GaAs_2$.

## Introduction

Lithium phosphidosilicates and -trielates became a highly interesting class of compounds in the last decade because of their structural features and ion conducting properties.[1,2,3,4] Compounds belonging to this class show isolated or condensed $MP_4$-tetrahedra ($M$ = Al, Ga, In, Si, Ge, Sn) as a standard structure feature. Recently, we have shown that $Li_3As$ exhibits mobile Li ions, similar to $Li_3P$, thus making arsenides a highly interesting substance class in terms of Li ion conducting materials.[5] The similarity to phosphides initiated the investigation of the ternary system Li–Si–As, where some compounds also show ion conductivity.[6,7] Since most of the known lithium arsenidosilicates show similar structural features as phosphide materials, the chemistry of phospidosilicates and arsenidosilicates seems to be quite comparable. The phosphidotrielates $Li_3TrP_2$ ($Tr$ = Al, Ga, In) were reinvestigated recently, but there is a lack of information concerning the corresponding arsenides.[8,9,10] We synthesized $Li_3AlAs_2$, reinvestigated the crystal structure and propose a new structure model isotypic to $Li_3AlP_2$. The heavier homologues $Li_3GaAs_2$ and $Li_3InAs_2$ were also synthesized, they are new members to this class of compounds. They all crystallize isotypic to the known, lighter phosphides. The layered anionic structure of $Li_3AlAs_2$ and $Li_3GaAs_2$ is the same as it is known for $Na_2LiInAs_2$, $K_2LiGaAs_2$ and $K_2LiInAs_2$, lithium environments differ.[11,12,13] Band structure calculations and impedance spectroscopy of $Li_3TrAs_2$ ($Tr$ = Al, Ga, In) reveal electronic properties from a theoretical and practical point of view.

## Results and Discussion

$Li_3AlAs_2$, $Li_3GaAs_2$ and $Li_3InAs_2$ were synthesized from the elements via ball milling and subsequent annealing at elevated temperatures. The compounds crystallize isotypic to the phosphides $Li_3AlP_2$, $Li_3GaP_2$ and $Li_3InP_2$. $Li_3InAs_2$ is the only $Li_3TrAs_2$ member that can also be synthesized phase pure from the elements without ball milling. The refined powder diffraction patterns (CuK$\alpha_1$ radiation, $\lambda$ = 1.540598 Å) are displayed in Figure 1.

$Li_3AlAs_2$ and $Li_3GaAs_2$ crystallize in the space group *Cmce* (No. 64), with $a$ = 11.894(1) Å, $b$ = 12.150(1) Å, $c$ = 6.005(1) Å, $V$ = 867.77(1) Å$^3$ and $Z$ = 8 for $Li_3AlAs_2$, and $a$ = 11.963(1) Å, $b$ = 12.163(1) Å, $c$ = 5.998(1) Å, $V$ = 872.77(1) Å$^3$ and $Z$ = 8 for $Li_3GaAs_2$. $Li_3InAs_2$ crystallizes in the space group $I4_1/acd$ (No. 142), with $a$ = 12.388(1) Å, $c$ = 24.659(1) Å, $V$ = 3784.19(2) Å$^3$ and $Z$ = 32. Refinement data is given in Table 1, Wyckoff positions, atom coordinates and displacement parameters are summarized in Table S1 in the supporting information. Structures were refined from powder diffraction data by the Rietveld method, using starting models of orthorhombic $Na_2LiGaAs_2$ and tetragonal $Li_2SiAs_2$, respectively. Missing lithium positions were found by Difference-Fourier synthesis. Refining structural models in higher symmetric space groups was not successful. The compounds crystallize isotypic to the known phosphides $Li_3AlP_2$, $Li_3GaP_2$ and $Li_3InP_2$. $Li_3AlAs_2$ and $Li_3GaAs_2$ show a layered structure. *Tr* occupies one half of the tetrahedral voids in a layer, the other half is occupied by lithium (Figure 2b). The layer without *Tr* atoms contains lithium in all tetrahedral voids (Figure 2 a)) The structures are visualized in Figure 2.

[a] F. Wegner, F. Kamm, Dr. F. Pielnhofer, Prof. Dr. A. Pfitzner
Institut für Anorganische Chemie
Universität Regensburg
Universitätsstraße 31, 93053 Regensburg
E-mail: arno.pfitzner@chemie.uni-regensburg.de

Supporting information for this article is available on the WWW under https://doi.org/10.1002/zaac.202200330



 

Journal of Inorganic and General Chemistry
ZAAC
Zeitschrift für anorganische und allgemeine Chemie





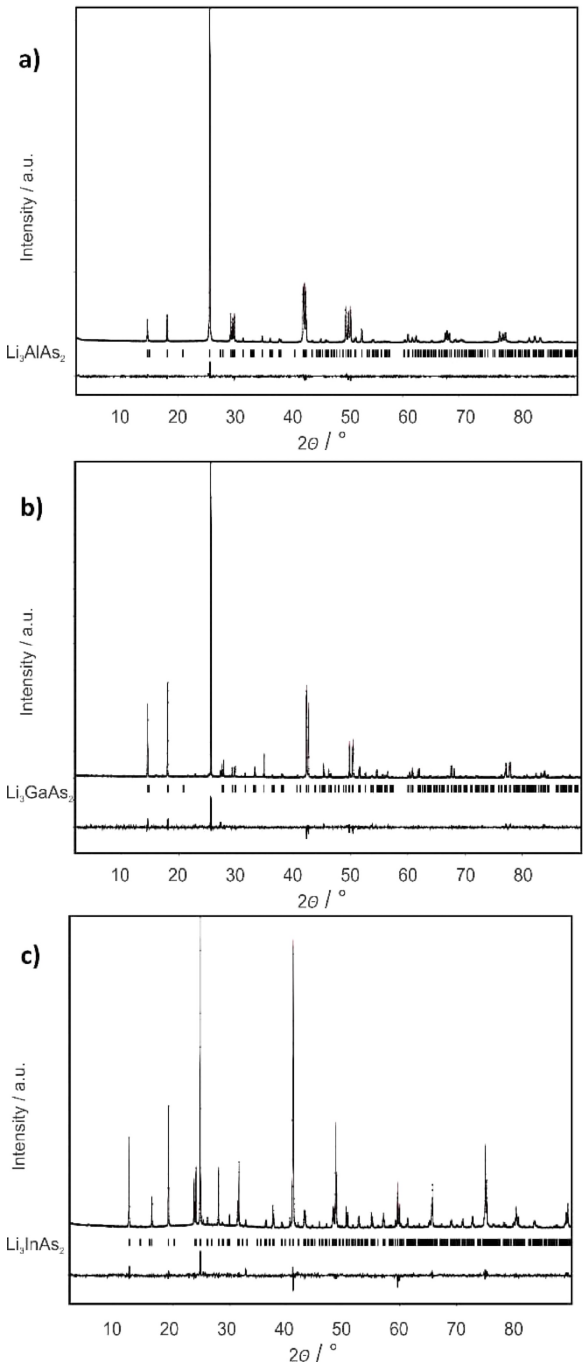


**Figure 1.** Refined powder diffraction patterns (measured and calculated) of $Li_3AlAs_2$ (a)), $Li_3GaAs_2$ (b)), and $Li_3InAs_2$ (c)) with difference plot using CuK$\alpha_1$-radiation at room temperature.

**Table 1.** Refinement parameters of $Li_3AlAs_2$, $Li_3GaAs_2$ and $Li_3InAs_2$ from Rietveld refinement at room temperature.

| Empirical formula | $Li_3AlAs_2$ | $Li_3GaAs_2$ | $Li_3InAs_2$ |
|---|---|---|---|
| *T*/K | | 293 | |
| Radiation wavelength | | λ = 1.540598 Å | |
| Θ range/deg. | | 2.00–91.185 | |
| Crystal system | | orthorhombic | tetragonal |
| Space group | *Cmce* (*No. 64*) | *Cmce* (*No. 64*) | *I41/acd* (*No. 142*) |
| Color | dark red | black | black |
| a/Å | 11.894(1) | 11.963(1) | 12.388(1) |
| *b*/Å | 12.150(1) | 12.163(1) | a |
| *c*/Å | 6.005(1) | 5.998(1) | 24.659(1) |
| *V*/Å3 | 867.77(1) | 872.77(1) | 3784.19(2) |
| *Z* | 8 | 8 | 32 |
| Formula weight/ g mol$^{-1}$ | 197.6 | 240.4 | 285.5 |
| $\rho$ (calc.)/g cm$^{-3}$ | 3.034 | 3.659 | 4.009 |
| $R_p$ | 0.0493 | 0.1179 | 0.0527 |
| $R_{wp}$ | 0.0633 | 0.1581 | 0.0688 |
| $R_{exp}$ | 0.0466 | 0.1452 | 0.0486 |
| $R_{gt}$, $wR_{gt}$ ($I > 3\sigma$) | 0.0252, 0.0282 | 0.0449, 0.0453 | 0.0375, 0.0406 |
| $R_{all}$, $wR_{all}$ | 0.0265, 0.0285 | 0.0568, 0.0476 | 0.0460, 0.0418 |
| $\Delta\rho_{min}$, $\Delta\rho_{max}$/eÅ$^{-3}$ | −0.36, 0.24 | −0.74, 0.79 | −0.69, 1.09 |
| *GOOF* | 1.36 | 1.09 | 1.42 |
| Depository no. | CSD-2210385 | CSD-2210386 | CSD-2210387 |

The bond distances in the $AlAs_4$-tetrahedra vary from *d*(Al–As1) = 2.478 Å to *d*(Al–As2) = 2.502 Å. All lithium positions are coordinated tetrahedrally by arsenic. Li1 in the tetrahedral voids of the $AlAs_4$-layer has bond distances of *d*(Li1–As1) = 2.591 Å and *d*(Li1–As2) = 2.659 Å). Li2 is located in all tetrahedral voids between the $AlAs_2$-layers with slightly different distances of *d*(Li2–As1) = 2.681 Å and *d*(Li2–As2) = 2.634 Å. $Li_3GaAs_2$ is isotypic to the aluminium compound. Bond distances in the $GaAs_4$-tetrahedra vary from *d*(Ga–As1) = 2.501 Å to *d*(Ga–As2) = 2.514 Å. Li1 in the tetrahedral voids of the $GaAs_4$-layer has bond distances of *d*(Li1–As1) = 2.613 Å and *d*(Li1–As2) = 2.657 Å. Li2 is located between the layers in all tetrahedral voids with slightly different distances of *d*(Li2–As1) = 2.695 Å and *d*(Li2–As2) = 2.578 Å. $Li_3InAs_2$ crystallizes isotypic to $Li_3InP_2$. $InAs_4$-tetrahedra form a supertetrahedral network as displayed in Figure 3. Indium is coordinated tetrahedrally with bond distances of *d*(In–As1) = 2.644 Å, *d*(In–As2) = 2.670 Å and *d*(In–As3) = 2.665 Å. Four tetrahedra form a $In_4As_{10}$-supertetrahedron that shares corners with the next supertetrahedron. The networks of supertetrahedra form interpenetrating rings as shown in Figure 3. Three independent lithium positions are located between the supertetrahedra, all of them are coordinated by four arsenic atoms in a distorted tetrahedral arrangement. Li–As distances are in the range of 2.343 Å (*d*(Li2–As2)) to 3.006 Å (*d*(Li1–As3)). Coordination polyhedra and corresponding bond lengths are given in the supporting information (Figures S1–S6).

Both crystal structures can be derived from a face centered cubic (*fcc*) aristotype structure type, as shown in Figure 4. The aristotype is the antifluorite structure. Arsenic atoms form a distorted cubic closest packing, lithium and the triel atoms occupy all tetrahedral voids, octahedral voids remain empty. Bärnighausen trees and splitting of the Wyckoff positions are shown in the supporting information (tables S2–S3). While $Li_3AlAs_2$ and $Li_3GaAs_2$ can be described as 2·2·1 superstructure

 

Journal of Inorganic and General Chemistry
ZAAC
Zeitschrift für anorganische und allgemeine Chemie





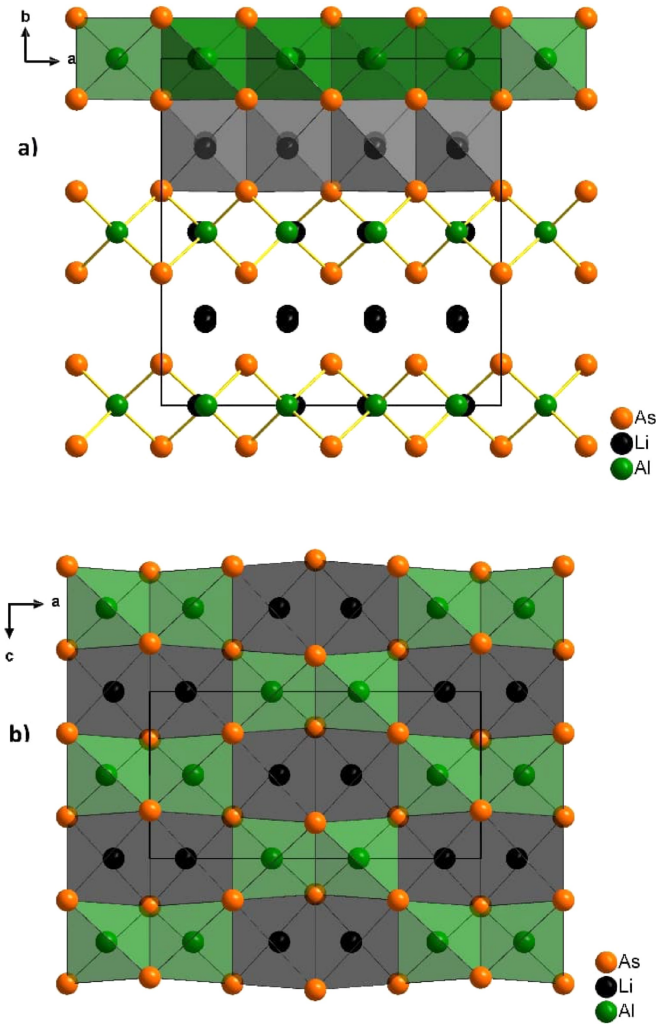


**Figure 2.** Crystal structure of orthorhombic $Li_3TrAs_2$ (*Tr* = Al, Ga) in *a-b-* (a)) and *a-c*-projection (b). A closest packing of arsenic with cations in all its tetrahedral voids. *Tr* atoms occupy 50 % of all tetrahedral voids in an *a-c-* layer, the other 50 % are occupied by lithium (b)). The layers without *Tr* atoms have lithium atoms in all of their tetrahedral voids (a)).

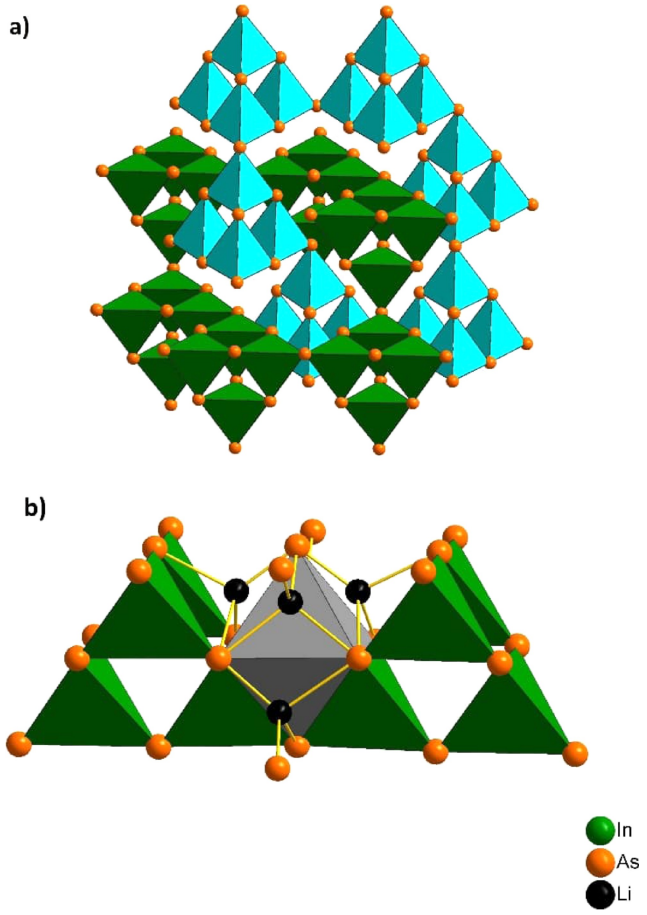


**Figure 3.** Structure picture of tetragonal $Li_3InAs_2$. Supertetrahedral networks of interpenetrating rings (identical networks visualized in different colors) (a)). 4 $InAs_4$-tetrahedra form supertetrahedra that are connected via common corners. Two independent supertetrahedral networks form interpenetrating rings. b): an empty octahedral void (grey) between two $In_4As_{10}$-supertetrahedra. The tetrahedrally coordinated lithium positions are strongly shifted towards the faces of the empty octahedra.

of the aristotype, a 2·2·4 supercell is needed for the description of $Li_3InAs_2$.

Thermal analyses of the compounds show several thermal effects. A reversible effect at about 770 °C for $Li_3AlAs_2$ (solid-solid phase transition or melting), numerous unclear effects for $Li_3GaAs_2$ above 550 °C and an effect at 550 °C for $Li_3InAs_2$ that could also be a solid-solid phase transition or melting. DTA curves are displayed in the supporting information (Figures S7–S9). Conductivity experiments were performed to check for ion mobility in the title compounds. Impedance spectroscopy in the temperature range of 50 °C–300 °C shows semiconducting behavior of $Li_3AlAs_2$, but ion mobility for $Li_3InAs_2$. $Li_3InAs_2$ shows a specific conductivity of $\sigma_{spec}$ (50 °C) = $7.3(1)\cdot10^{-7}$ S·cm$^{-1}$ to $\sigma_{spec}$ (300 °C) = $5.3(1)\cdot10^{-5}$ S·cm$^{-1}$ and an activation energy of 0.43(4) eV which is in a common range for arsenide-based lithium-ion conductors.[6,7] Arrhenius plot and activation energy are displayed in Figure 5. In contrast, $Li_3AlAs_2$ shows only electronic conductivity in the range of $\sigma_{spec}$ (50 °C) = $8(1)\cdot10^{-5}$ S·cm$^{-1}$ to $\sigma_{spec}$ (300 °C) = $3.2(6)\cdot10^{-4}$ S·cm$^{-1}$ and a very low activation energy of 0.09(5) eV. We are unable to distinguish conductivity data of $Li_3GaAs_2$ in semi- or ion conducting. Nyquist plots are given in the supporting information (Figure S11). In all three compounds all tetrahedral voids are fully occupied. 100 % occupied voids make hopping processes less favorable. All lithium atoms are coordinated tedrahedrally, but in $Li_3InAs_2$ the $LiAs_4$ tetrahedra are heavily distorted, compared to lighter homologues as shown in the supporting information. The heavier homologue $Li_3InAs_2$ shows moderate ion conductivity, in contrast to $Li_3InP_2$, which shows only electronic charge transport properties. In $Li_3InP_2$, the coordination of $Li^+$ is a slightly distorted tetrahedron. The distances *d*(Li–P) in $Li_3InP_2$ are in the range of 2.526 Å to 2.673 Å. In $Li_3InAs_2$ the corresponding distances vary from 2.343 Å to 3.006 Å. The lithium positions are shifted towards a

 

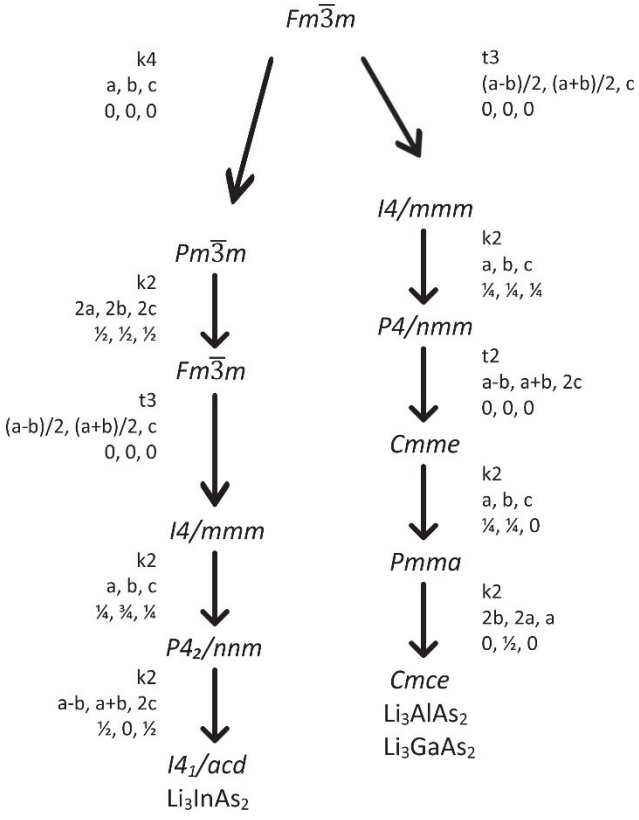


**Figure 4.** Group-subgroup scheme for symmetry relations of $Li_3TrAs_2$ modifications. Both modifications can be derived from the cubic antifluorite-type structure (SG *Fm*$\bar{3}$*m*, No. 225).

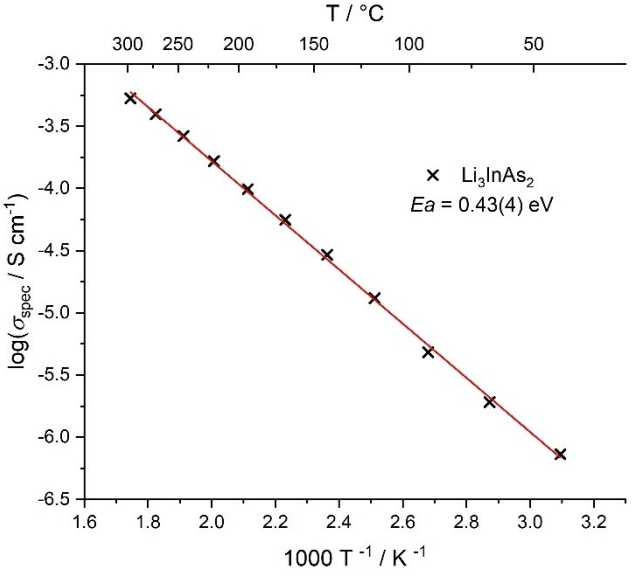


**Figure 5.** Arrhenius plot from impedance spectroscopy of ion conducting $Li_3InAs_2$. The activation energy of 0.43(4) eV is in the range of other lithium - ion conducting arsenides.

face of the tetrahedron with an empty octahedral void on the backside of this face (see Figure 3b)). This could be a reason for higher lithium-ion mobility in a supertetrahedral framework like $Li_3InAs_2$. We could not find any additional electron density corresponding to lithium positions in octahedral voids or other disorder via the Rietveld refinements. In literature it is mentioned that ionic conductivity rises with the size of supertetrahedral networks .[14] More sophisticated experiments as low-temperature single crystal diffraction or neutron powder diffraction might give more information on the lithium-ion distribution in these compounds. As band structure calculations show a small band gap matching the black color of the compound, we cannot exclude a partial electronic contribution to the total conductivity measured in our experiments. The isotypic compounds $Li_3AlAs_2$, $Li_3GaAs_2$, $Li_3AlP_2$ and $Li_3GaP_2$ do not show ion mobility, because tetrahedral voids are fully occupied, and lithium-ion hopping is hindered. The layered structure of the lighter homologues could enhance electronic conductivity parallel to the *a*-*c*-plane. Anyhow, the structurally related compounds $Li_2SiN_2$, $Li_2SiP_2$, $Li_2GeP_2$, $Li_2SiAs_2$ and $Li_2GeAs_2$ show ion mobility, what is due to a small occupation of octahedral voids by lithium.[15,16,17,7] These compounds also feature supertetrahedral networks of condensed $TtPn_4$-tetrahedra (*Tt* = Si, Ge; *Pn* = N, P, As) similar to $Li_3InAs_2$.

DFT calculations were performed to determine the electronic structures of $Li_3TrAs_2$. All three compounds are direct band gap semiconductors with band gaps of 2.79 eV ($Li_3AlAs_2$), 1.87 eV ($Li_3GaAs_2$) and 2.13 eV $Li_3InAs_2$ as shown in Figure 6. The calculated band gaps are in line with the color of the compounds.

## Conclusion

We report on the solid-state synthesis and characterization of phase pure $Li_3AlAs_2$, $Li_3GaAs_2$ and $Li_3InAs_2$. The arsenidotrielates crystallize isotypic to known phosphidotrielates. Their crystal structures can be derived from the antifluorite structure type via a Bärnighausen tree. The title compounds are direct band gap semiconductors. Impedance measurements show high electric conductivity for layered $Li_3AlAs_2$ and moderate ionic conductivity for supertetrahedral $Li_3InAs_2$. Syntheses and characterization of more ternary main group compounds containing lithium and arsenic are scheduled.

## Experimental Section

As arsenic and its compounds are very toxic and arsenic vapor pressure strongly correlates to the temperature, additional safety considerations concerning the synthesis procedure are highly recommended. All manipulations were carried out in a Glovebox (M Braun) with oxygen and $H_2O$ levels below 0.5 ppm. All compounds can be synthesized by ball milling of stoichiometric amounts of the elements lithium (Merck, 99%), aluminium (chempur, 99.9%), gallium (chempur, 99.9%), indium (alfa, 99%) and arsenic (chempur, 99%). Lithium was used in small excess (5%) to compensate for evaporation loss. For homogenization a FRITSCH Pulverisette 7 premium line equipped with 25 mL zirconia grinding bowls and 10 grinding balls (Ø = 10 mm) was used. Milling for about 3 h at a top speed of 600 rpm leads to a reactive mixture of the elements.

 

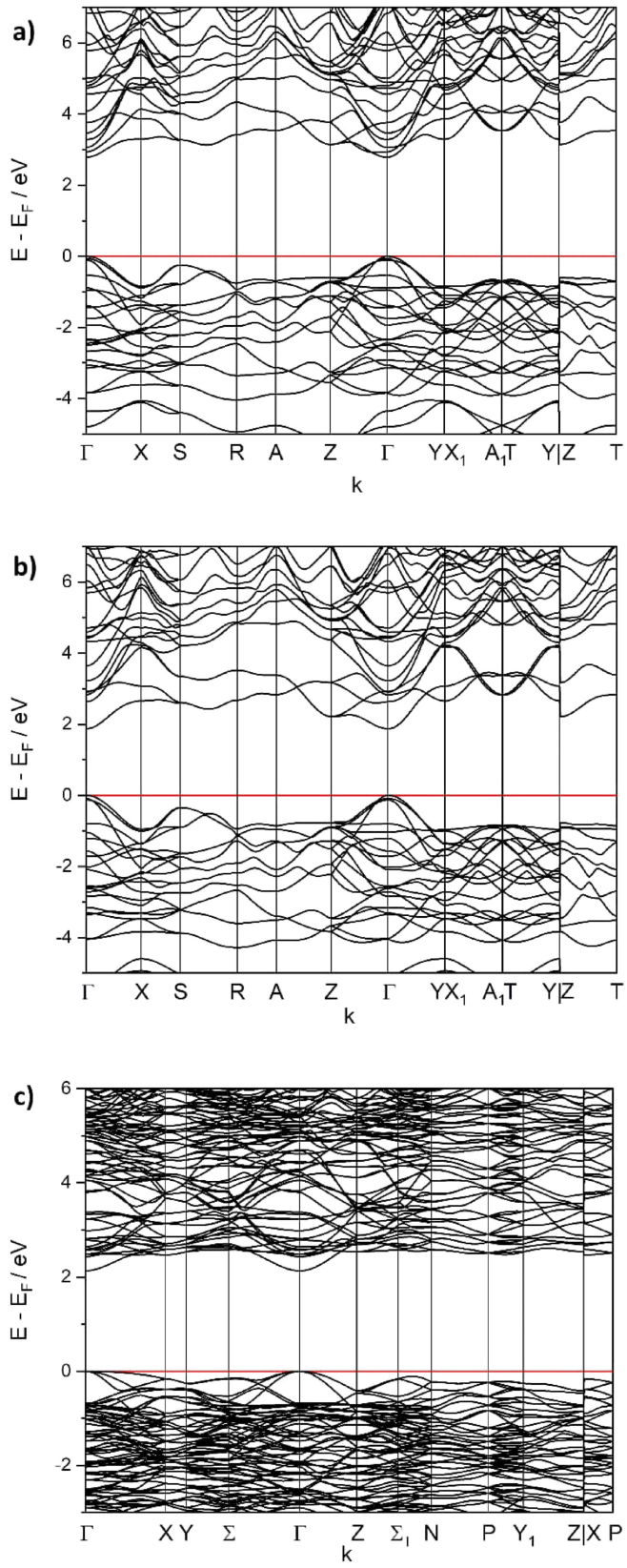


**Figure 6.** Band structures of $Li_3TrAs_2$ with band gaps of around 2.79 eV ($Li_3AlAs_2$ (a)), 1.87 eV $Li_3GaAs_2$ (b)), and 2.13 eV $Li_3InAs_2$ (c)).

0.5 g of this reactive mixture were placed in a graphite container (Ø = 6 mm) that was closed with a lid. The container was encapsulated in an Ar flushed and subsequently evacuated silica ampoule and heated to 600 °C ($Li_3AlAs_2$), 500 °C ($Li_3GaAs_2$) and 650 °C ($Li_3InAs_2$), respectively, for about two days. $Li_3InAs_2$ was also obtained by direct reaction of lithium and indium pieces covered by arsenic powder in a graphite crucible. The sample was heated to 650 °C for 3 days, reground and heated to 700 °C for 3 days again. The products of the annealed ball milled mixture and the direct synthesis process are equivalent. All compounds are moisture sensitive and release $AsH_3$ when getting in contact with humid air or water. $Li_3AlAs_2$ is a dark red powder, $Li_3GaAs_2$ is slightly darker and $Li_3InAs_2$ is black. DTA: the samples were encapsulated in quartz tubes (Ø = 2 mm) and sealed under vacuum. A SETRARAM TG-DTA 92.16.18 was used to investigate thermal properties up to 800 °C. $Li_3AlAs_2$ shows a reversible effect at about 770 °C, $Li_3GaAs_2$ shows numerous effects that cannot be clearly interpreted and $Li_3InAs_2$ shows melting or a phase transition at around 550 °C. Powder diffraction: finely ground samples were filled in quartz capillaries (Ø = 0.3 mm for $Li_3AlAs_2$ and $Li_3GaAs_2$; 0.2 mm for $Li_3InAs_2$) that were flame sealed to protect hydrolysis during the measurement. Capillaries were mounted on a STOE STADI P diffractometer (Stoe & Cie) equipped with a Mythen 1 K detector for data collection and an optional graphite furnace for high temperature measurements. CuK$\alpha_1$-radiation was used in all measurements. Raw data was processed with the *WinXPOW* software package (Stoe & Cie), *Jana2006* was used for Rietveld refinements.[18,19] Impedance spectroscopy: To determine conductivity behavior impedance experiments were performed using a Zahner Zennium impedance analyzer coupled with an in-house built furnace in a glovebox. Samples were cold-pressed (Ø = 8 mm) and contacted with gold foil. Measurements from 50–300 °C in the frequency range from 1 MHz to 100 mHz showed ion conductivity for $Li_3InAs_2$ and electronic transport phenomena for $Li_3AlAs_2$. Data for $Li_3GaAs_2$ was not clear. As our glovebox cannot be cooled actively, room temperature measurements remain difficult. The software *Zahner Analysis* was used for data processing and fitting.[20] DFT modelling: calculations were performed using the CRYSTAL17 code.[21,22] Basis sets were taken from the literature.[22,23,24,25,26] Full structure optimizations were done starting from structure models obtained by Rietveld refinements. For all calculations the HSE06 functional with a k-mesh sampling of 6·6·6 was used and the convergence criteria was set to $10^{-8}$ atomic units.[27,28] Band structures were computed for all compounds using k-paths proposed by Setyawan and Curtarolo.[29] The high symmetry points were calculated using the seeK-path online tool.[30]

## Acknowledgements

The authors express their gratitude to the Free State of Bavaria and the University of Regensburg for excellent working conditions. Open Access funding enabled and organized by Projekt DEAL.

## Conflict of Interest

The authors declare no conflict of interest.

## Data Availability Statement

The data that support the findings of this study are available in the supplementary material of this article.

**Keywords:** arsenidotrielates · band gap calculation · impedance spectroscopy · DFT modelling · semiconductor

[1] A. Haffner, T. Bräuniger, D. Johrendt, *Angew. Chem. Int. Ed.* **2016**, *55*, 13585–13588; *Angew. Chem.* **2016**, *128*, 13783–13786.
[2] S. Strangmüller, H. Eickhoff, G. Raudaschl-Sieber, H. Kirchhain, C. Sedlmeier, L. van Wüllen, H. A. Gasteiger, T. F. Fässler, *Chem. Mater.* **2020**, *32*, 6925–6934.
[3] H. Eickhoff, S. Strangmüller, W. Klein, H. Kirchhain, C. Dietrich, W. Zeier, L. van Wüllen, T. F. Fässler, *Chem. Mater.* **2018**, *30*, 6440–648.
[4] T. M. F. Restle, C. Sedlmeier, H. Kirchhain, W. Klein, G. Raudaschl-Sieber, V. L. Deringer, L. van Wüllen, H. A. Gasteiger, T. F. Fässler, *Angew. Chem. Int. Ed.* **2020**, *27*, 5665–5674.
[5] F. Wegner, F. Kamm, F. Pielnhofer, A. Pfitzner, *Z. Anorg. Allg. Chem.* **2022**, *648*, e202100358.
[6] J. Mark, K. Lee, M. A. T. Marple, S. Lee, S. Sen, K. Kovnir, *J. Mater. Chem. A.* **2020**, *8*, 3322–3332.
[7] Claudia De Giorgi, *Dissertation*, **2021**, University of Regensburg.
[8] T. M. F. Restle, J. V. Dums, G. Raudaschl-Sieber, T. F. Fässler, *Chem. Eur. J.* **2020**, *26*, 6812–6819.
[9] T. M. F. Restle, V. L. Deringer, J. Meyer, G. Raudaschl-Sieber, T. F. Fässler, *Chem. Sci.* **2021**, *12*, 1278–1285.
[10] R. Juza, W. Schulz, *Z. Anorg. Allg. Chem.* **1952**, *269*, 1–12.
[11] M. Somer, W. Carillo-Cabrera, E.-M. Peters, K. Peters, H. G. von Schnering, *Z. Kristallogr.* **1995**, *210*, 877.
[12] M. Somer, W. Carillo-Cabrera, E.-M. Peters, K. Peters, H. G. von Schnering, *Z. Kristallogr.* **1994**, *210*, 528.
[13] M. Somer, W. Carillo-Cabrera, E.-M. Peters, K. Peters, H. G. von Schnering, *Z. Kristallogr.* **1995**, *210*, 959.
[14] A. Haffner, A–K. Hatz, I. Moudrakowski, B. V. Lotsch, D. Johrendt, *Angew. Chem. Int. Ed.* **2018**, *21* 6263–6268.
[15] S. Pagano, M. Zeuner, S. Hug, W. Schnick, *Eur. J. Inorg. Chem.* **2009**, *12*, 1579–1584.
[16] L. Toffoletti, H. Kirchhain, J. Landesfeind, W. Klein, L. van Wüllen, H. A. Gasteiger, T. F. Fässler, *Chem. Eur. J.* **2016**, *22*, 17635–17645.
[17] H. Eickhoff, C. Sedlmeier, W. Klein, G. Raudaschl-Sieber, H. A. Gasteiger, T. F. Fässler, *Z. Anorg. Allg. Chem.* **2019**, *646*, 95–102.
[18] STOE-WinXPOW, *Vol. Version 3.0.2.5*, Stoe & Cie GmbH Darmstadt, **2011**.
[19] V. Petricek, M. Dusek, *Z. Kristallogr.* **2014**, *229*, 345.
[20] Zahner-Meßtechnik GmbH & Co. KG, *Vol. Version Z.3.03*, Thales Flink, Kronach.
[21] R. Dovesi, A. Erba, R. Orlando, C. M. Zicovich-Wilson, B. Civalleri, L. Maschio, M. Rerat, S. Casassa, J. Baima, S. Salustro, B. Kirtman, *WIREs Comput. Mol. Sci.* **2018**, *8*, e1360.
[22] R. Dovesi, V. R. Saunders, C. Roetti, R. Orlando, C. M. Zicovich-Wilson, F. Pascale, B. Civalleri, K. Doll, N. M. Harrison, I. J. Bush, P. D'Arco, M. Llunell, M. Causà, Y. Noël, L. Maschio, A. Erba, M. Rerat, S. Casassa, *CRYSTAL17 User's Manual*, University of Torino: Torino, **2017**.
[23] M. F. Peintinger, D. Vilela Oliveira, T. Bredow, *J. Comput. Chem.* **2013**, *34*, 451–459.
[24] B. Montanari, B. Civalleri, C. M. Zicovich-Wilson, R. Dovesi, *Int. J. Quantum Chem.* **2006**, *106*, 1703–1714.
[25] R. Pandey, J. E. Jaffe, N. M. Harrison, *J. Phys. Chem. Solids* **1994**, *55*, 1357–1361.
[26] M. Causà, R. Dovesi, C. Roetti, *Phys. Rev. B* **1991**, *43*, 11937–11943.
[27] A. D. Becke, *Phys. Rev. A* **1988**, *38*, 3098.
[28] J. Heyd, G. E. Scuseria, M. Ernzerhof, *J. Chem. Phys.* **2003**, *118*, 8207.
[29] W. Setyawan, S. Curtarolo, *Comput. Mater. Sci.* **2010**, *49(2)*, 299–312.
[30] Y. Hinuma, G. Pizzi, Y. Kumagai, F. Oba, I. Tanaka, *Comp. Mat. Sci.* **2017**, *128*, 140.

Manuscript received: October 7, 2022
Revised manuscript received: November 10, 2022
Accepted manuscript online: November 18, 2022

 